Available online at www.sciencedirect.com
SCIENCE DIRECT®
Physics and Chemistry of the Earth 29 (2004) 277–286
PHYSICS and CHEMISTRY of the EARTH
www.elsevier.com/locate/pce

Improved radio occultation sounding of the Arctic atmosphere using simulations with a high resolution atmospheric model

V. Kunitsyn [a], V. Zakharov [a], K. Dethloff [b], A. Weisheimer [b], M. Gerding [b], R. Neuber [b,*], A. Rinke [b], I. Hebestadt [b]

[a] *M. Lomonosov Moscow State University, Russia*
[b] *Alfred Wegener Institute for Polar and Marine Research, Physical and Chemical Processes in the Atmosphere, Telegrafenberg A43, Potsdam 14473, Germany*

Abstract

Radio occultation experiments have been simulated for the Arctic region on the basis of the regional atmospheric model HIRHAM4. Irregular structures in the atmosphere produce a violation of the quasi-sphericity in the radio signal propagation and exert a strong influence on the accuracy of atmospheric profiles retrieved by the radio occultation technique. Errors in radio occultation data are spatially localised and associated with gradients in atmospheric structures. Local errors reach 2% in retrieved profiles of refractivity corresponding to an error of 6 K in temperature. Therefore mesoscale variations in atmospheric parameter gradients in a specified region must be taken into account when interpreting radio occultation data.

We show, that a correction functional can be developed using the refractivity index field calculated from the regional model in order to improve the radio occultation retrieval of atmospheric parameters. This functional is constructed from instantaneous model outputs, as well as from temporally averaged fields of refractivity using data of the HIRHAM4 model for the Arctic atmosphere. The correction functional derived from monthly averaged data reduced the retrieval errors of refractivity, temperature, and pressure in the troposphere, in particular, temperature retrieval errors are reduced up to 1 K. Application of this kind of functional depends on whether the model used for the construction of the functional is able to simulate the real mesoscale atmospheric structures.

1. Introduction

Satellite radio occultation (RO) data are effectively used for the derivation of vertical profiles of meteorological parameters and for the estimation and verification of meteorological data and Earth climate models. Low-orbiting satellites with GPS receivers, like GPS/MET, CHAMP and Oersted, allow to reconstruct profiles of atmospheric parameters by means of the occultation technique. Of particular importance is the use of the occultation techniques in the Arctic region due to coarse observational data.

A classical method for the profile reconstruction is based on the Abel transform, assuming a quasi-spherical atmosphere. The reconstructed atmospheric profiles of a non-spherical atmosphere are ''averaged-weighted'' profiles. A comparison of the capabilities of the various diagnostic systems was performed by Gorbunov and Kornblueh (2001). If the employed atmospheric model adequately describes the real atmosphere, the calculated profiles will agree with the experimental ones. The comparison of the ''averaged'' profiles with the experimental ones allows to intercompare different models of the atmosphere and to verify and validate the data produced by these models. Also other methods exist for such a data analysis, for example the non-linear optimal estimation inverse method (Palmer et al., 2000) and the four-dimensional variation (4Dvar) method (Zou et al., 1999).

When RO data are used, reconstructed height profiles of the refraction index and corresponding atmospheric parameters are contaminated by errors. Significant error sources are tropospheric gradients in the atmospheric fields, multi-path propagation of the signal due to the complex mesoscale structure of the humidity field, influence of the ionosphere and irregular ionospheric structures. The appearance of multi-path propagation is typical for tropical regions where most of the occultations observed by the GPS/MET and CHAMP missions

* Corresponding author. Tel.: +49-331-288-2129; fax: +49-331-288-2178.
E-mail addresses: dethloff@awi-potsdam.de (K. Dethloff), neuber@awi-potsdam.de (R. Neuber).

1474-7065/$ - see front matter © 2004 Elsevier Ltd. All rights reserved.
doi:10.1016/j.pce.2004.01.012

do not reach the Earth's surface. In the Arctic region, however, the atmospheric humidity is generally low and multi-path propagation is encountered quite seldom. Due to this fact, the quality of tropospheric data is much higher in the Arctic.

The most significant error source for the reconstruction of atmospheric parameters in the Arctic troposphere are horizontal gradients. These gradients will be discussed in the present paper. The analysis is carried out by means of numerical simulations based on the regional model HIRHAM4 that has a high horizontal resolution in space (see Fig. 1) and time. The Arctic region is marked by a pronounced orography with mesoscale features. This orography is used in the model and allows the realistic examination of radio occultations. The error sources including horizontal gradients in the atmosphere were previously discussed in some publication (e.g. Kursinski et al., 1995, 1997; Bengtsson et al., 1996; Rocken et al., 1997; Gorbunov and Sokolovskiy, 1993, 2001; Zou et al., 1999; Healy, 2001; Palmer et al., 2000; Healy and Eyre, 2000).

Here we propose the methods to correct vertical atmospheric profiles by using the instantaneous or averaged field of index of refraction produced by the HIRHAM4 model. The presence of irregular structures in the region under study is characterised by gradients in the corresponding fields. A series of different approaches for GPS data analysis and/or assimilation have been proposed earlier. Such general approaches are based on minimizing the corresponding functionals including the measured refraction angle, or the difference between model and retrieved values of refractivity (Zou et al., 1999). However, in some regions where refraction fields have comparatively stable spatial structures with typical gradients, simplified approaches to the correction procedure are applicable. Such a simplified approach is proposed here, involving no variation procedures that require considerable computation time. Our approach is based on the construction of a correction functional using the HIRHAM4 model data. Applying this functional to real experimental data depends on whether the model is able to simulate the real mesoscale atmospheric structure.

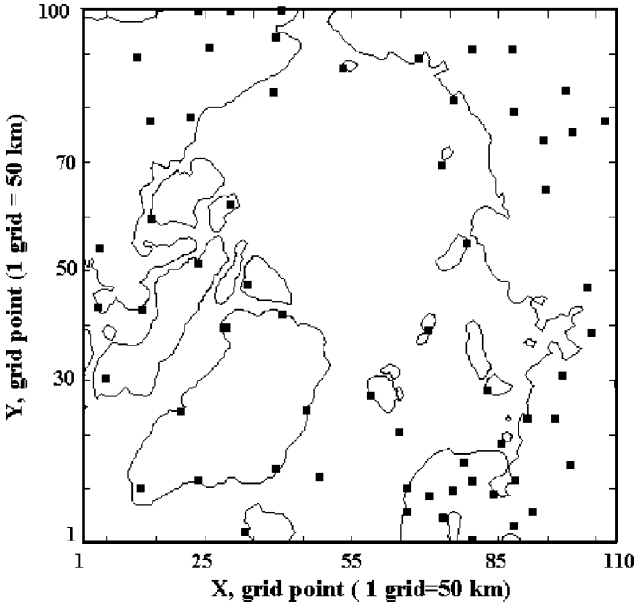

Fig. 1. The area covered by the regional model HIRHAM4. Black squares indicate the locations of weather stations. x- and y-axes give the indices of the model grid points. The model covers an area of 5500×5000 km which corresponds to 110×100 grid points. The point $(1,1)$ has the coordinates (53.5° N; 44.72° W), the point $(110,1)$ has coordinates (53.85° N; 44.23° E), the point $(1,100)$ has coordinates (53.82° N; 134.62° W), and the point $(110,100)$ has coordinates (53.17° N; 135.11° E).

2. Regional atmospheric model HIRHAM

Dethloff et al. (1996) and Rinke et al. (1999) integrated the regional atmospheric model of the Arctic HIRHAM4 with a high horizontal resolution of around 50 km. This model was driven at the lateral and lower boundaries by time-dependent ERA data (Gibson et al., 1997). It captures the horizontal mesoscale structures of atmospheric circulation patterns and storm tracks with very high accuracy, as estimated in Dethloff et al. (2002). They showed that the HIRHAM4 model reasonably represents the synoptic situations that lead to precipitation in the Arctic and around Greenland. Maxima of precipitation and accumulation occur at the south-western and south-eastern coasts of Greenland and are connected with cyclonic activity and the main storm tracks around Greenland. The state-of-the-art model HIRHAM4 represents the spatial variations of Greenland precipitation quite realistically since it is able to reasonably represent the synoptic situations that lead to precipitation.

Further results of model simulations in the Arctic, the validation against ECMWF analyses and station data, and intercomparison with the regional model ARCSyM over the Arctic were described by Dethloff et al. (1996), Rinke et al. (1997, 1999, 2000), and Kattsov et al. (2000). The sensitivity of the Arctic atmospheric simulations to initial and boundary conditions was investigated in Rinke and Dethloff (2000).

The following output parameters of the model have been used:

1. The field of the atmospheric pressure $p_{ij}^{(0)}$ in σ-coordinates that allows to compute the pressure at 19 vertical levels of the model up to 25 km height, in accordance with the equation $p_{ij}^{(k)} = \sigma_k \cdot p_{ij}^{(0)}$ where the pressure at the level k in the grid point (i,j) is defined through the pressure at the ground level and the coefficients σ_k given in the model, while $1 \leqslant i \leqslant 110$, $1 \leqslant j \leqslant 100$ and $0 < k \leqslant 19$.

2. The fields of temperature $T_{ij}^{(k)}$ and humidity $w_{ij}^{(k)}$ at the same 19 model levels are provided with a 6-h temporal resolution.

The system of equations of momentum, heat, state and continuity used in the model is solved on a horizontal grid with a 50 km mesh. The area covered by the model in the Arctic region is 5500×5000 km which corresponds to 110×100 points. Geographic coordinates of the HIRHAM4 region are indicated in Fig. 1. The point $(1,1)$ has the coordinates (53.5° N; 44.72° W), the point $(110,1)$ has coordinates (53.85° N; 44.23° E), the point $(1,100)$ has coordinates (53.82° N; 134.62° W), the point $(110,100)$ has coordinates (53.17° N; 135.11° E), and the point $(56,51)$ corresponds to the North Pole.

Positions of main weather stations are shown in Fig. 1 by small squares. Radio occultation data is recorded in this region currently by two satellites, Oersted and CHAMP. They can provide data with high temporal and spatial resolution in this region.

3. The radio occultation method

The RO method is known as a source of information about the height profile of the refraction index (Fjeldbo and Eshleman, 1965; Phinney and Anderson, 1968). In the simplest scheme of the occultation technique, one satellite is observing radio rise or radio set of another one, which carries a transmitter of electromagnetic waves. In the experiment the amplitude and group delays are measured as well as phase delays, that are connected with the Doppler refraction frequency shift on the GPS frequencies of $L_1 = 1.57542$ GHz and $L_2 = 1.2276$ GHz. The vertical profile of the refraction angle is related to the profile of the refraction index through the Abel transform under the assumption of spherical symmetry. From the latter one can obtain the height profiles of density, temperature and pressure in the atmosphere and the electron concentration in the ionosphere.

This method is of special importance for monitoring the state of the atmosphere (Kursinski et al., 1995; Rocken et al., 1997; Kursinski et al., 1997) and the ionosphere (Leitinger et al., 1997; Hajj and Romans, 1998; Schreiner et al., 1999; Syndergaard, 2000).

The simulation scheme takes into account the influence of inhomogeneous atmospheric and ionospheric structures on the signal (Vorob'ev and Krasilnikova, 1993; Gorbunov, 1994, Zakharov and Kunitsyn, 1998), and multi-path propagation in the media (Gorbunov and Gurvich, 1998; Zakharov and Kunitsyn, 1999; Gorbunov, 2001). The wave optics approach was used by Gorbunov (2001) and Gorbunov and Kornblueh (2001) to reproduce more accurately multi-path propagation effects.

3.1. Solution of the forward problem

The equation for the ray propagating in a medium with a spatial distribution of the refraction index $n(\vec{r})$ in Cartesian coordinates takes the well known form

$$\frac{\mathrm{d}^2\vec{r}}{\mathrm{d}\tau^2} = n\nabla n, \tag{1}$$

where the introduced symbols are used in ordinary sense: the coordinate vector $\vec{r}(\tau) = \{x(\tau), y(\tau), z(\tau)\}$ of a ray trajectory is defined by the parameter τ, $\mathrm{d}\tau = \mathrm{d}s/n$, where s is the coordinate along the length of the ray path. Eq. (1) can be solved for a given distribution of $n(\vec{r})$ numerically by means of a Runge–Kutta–Feldberg method of 4th order with an adaptive choice of the integration step (Forsythe et al., 1977). Boundary conditions are defined by the position of the satellites. The refraction angle α is determined as the angle between vectors tangential to the trajectory in the points of satellite locations of the GPS transmitter and the low earth orbital receiver (LEO). The superscript t denotes the tangential component of the vector, where the roof sign denotes the angle between the vectors, see Fig. 2.

$$\alpha(p) = (\widehat{\vec{u}^{\mathrm{t}}_{\mathrm{GPS}}, \vec{u}^{\mathrm{t}}_{\mathrm{LEO}}}). \tag{2}$$

The impact parameter p is obtained from the ray refraction law, and the formula for determining this parameter can be written as

$$\begin{aligned} p &= n(\vec{r}_{\mathrm{GPS}}) \cdot |\vec{r}_{\mathrm{GPS}} \times \vec{u}^{\mathrm{t}}_{\mathrm{GPS}}| \\ &= n(\vec{r}_{\mathrm{LEO}}) \cdot |\vec{r}_{\mathrm{LEO}} \times \vec{u}^{\mathrm{t}}_{\mathrm{LEO}}|, \end{aligned} \tag{3}$$

and, with sufficient accuracy, one can set $n(\vec{r}_{\mathrm{LEO}}) = n(\vec{r}_{\mathrm{GPS}}) = 1$. Calculations of the Doppler shift were carried out in accordance with Vorob'ev and Krasilnikova (1993) for each operating frequency transmitted from the GPS satellite. The error in simulating the forward problem was determined from the relative error of the integration and was less than 10^{-10}. This value corresponds to an absolute value less than 2–3 mm. In the

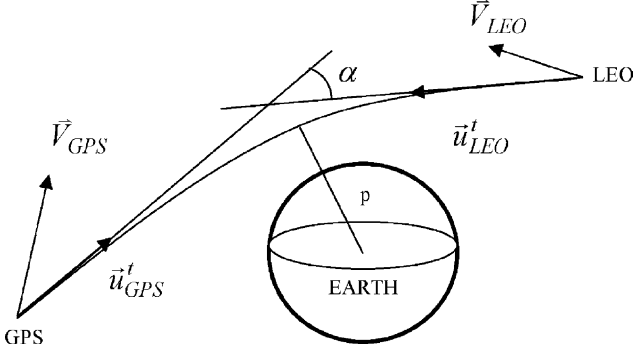

Fig. 2. The geometric scheme of a radio occultation. "GPS" indicates the GPS satellite with the sender, "LEO" indicates the Low Earth Orbiter satellite with the GPS receiver, α gives the refraction angle (see text).

case of a spherically symmetric medium, this error will produce a 0.1% reconstruction error for the profiles of atmospheric parameters.

3.2. Calculation of the refraction index field

To solve Eq. (1), one has to define the spatial field of the refraction index distribution $n(\vec{r})$. The atmospheric output fields from the HIRHAM4 model were used. They include fields of pressure $p_{ij}^{(k)}$, temperature $T_{ij}^{(k)}$, and humidity $w_{ij}^{(k)}$ at all 19 height levels at altitudes up to 25 km.

The refraction indices at the grid points of the model can be calculated in accordance with the known relationship (Bean and Dutton, 1968)

$$n_{ij}^{(k)} = 1 + N_{ij}^{(k)} = 1 + c_1 \cdot \frac{p_{ij}^{(k)}}{T_{ij}^{(k)}} + c_2 \frac{p_{Wij}^{(k)}}{\left(T_{ij}^{(k)}\right)^2}, \tag{4}$$

where the numerical values of the parameters are $c_1 = 7.76 \cdot 10^{-5}$ K hPa^{-1}, $c_2 = 0.373$ K^2 hPa^{-1}. Function $p_{W,ij}^{(k)}$ which describes the water vapour pressure at a given temperature $T_{ij}^{(k)}$ and humidity $w_{ij}^{(k)}$ is defined as

$$p_{W,ij}^{(k)} = \frac{w_{ij}^{(k)} \cdot p_{ij}^{(k)}}{R_{\mathrm{dw}} + (1 - R_{\mathrm{dw}}) \cdot w_{ij}^{(k)}},$$

where $R_{\mathrm{dw}} = R_{\mathrm{d}}/R_{\mathrm{w}} = 0.622$ is a ratio of the gas constant for dry air R_{d} to that for humid air R_{w}.

To determine the geometric height z in the atmosphere, a reference geoid was used in the model. Geometrical difference in altitudes between two height levels $z_2 - z_1$ for the pressure levels $p(z_1)$ and $p(z_2)$ set in a model respectively, are determined as (Wallace and Hobbs, 1977)

$$z_2 - z_1 = \int_{P_1}^{P_2} R_{\mathrm{d}} \cdot g(z, \varphi, \lambda) T \frac{\mathrm{d}p}{p}, \tag{5}$$

where $g(z, \varphi, \lambda)$ is the gravity acceleration as a function of the height z, latitude φ and longitude λ.

The height dependencies of the calculated refraction index were obtained for each grid point (i, j). In the calculated height profiles, certain basic height levels have been chosen, to provide convenience for further processing and to minimize the interpolation errors. The number of levels can vary within some limits but does not exceed 32. The refraction index values at these levels for a fixed grid point (i, j) are determined by a cubic spline function built over the whole ensemble of the data obtained in accordance with (5). Outside the region where the data were delivered by the HIRHAM model, CIRA data were used up to 80 km altitudes (Rees, 1988). Ionospheric influences are considered by using the IRI-95 model (Bilitza, 1990; http://nssdc.gsfc.nasa.gov/space/model/models/iri.html).

To calculate the ray trajectory when solving Eq. (1), it is necessary to obtain the refraction index values at an arbitrary point inside the region described in the HIRHAM model. For this purpose, a bicubic spline interpolation scheme (Ahlberg et al., 1967) was constructed on the spatial grid of the data for their approximation. The used approximation provides continuous values of the function $n(\vec{r})$ and its first derivatives $\frac{\partial n(\vec{r})}{\partial x}$, $\frac{\partial n(\vec{r})}{\partial y}$, $\frac{\partial n(\vec{r})}{\partial z}$.

3.3. Solution of the inverse problem

In modelling the forward problem (1)–(3), the dependencies of the refraction angle α on the impact parameter p were obtained for two sounding frequencies. Correction for the ionospheric influence on reconstructing the atmospheric profile was carried out using the two-frequency method (Vorob'ev and Krasilnikova, 1993). The use of the Abel transform assuming spherical symmetry of the atmosphere allows the reconstruction of the height profile of the refraction index (Fjeldbo and Eshleman, 1965; Phinney and Anderson, 1968),

$$n_i(a) = \exp\left[\frac{1}{\pi}\int_a^H \frac{\alpha_i(p)\,\mathrm{d}p}{\sqrt{p^2 - a^2}}\right], \quad a = r n_i(z), \tag{6}$$

where $H \geqslant 80$ km is the upper boundary. The inverse problem was solved according to the known relationship (6), which comprises the reconstruction of the height profiles of the parameters of the neutral atmosphere and of the electron concentration in the ionosphere. Local hydrostatic equilibrium was assumed and the equation of state was used. The obtained profiles of $n(x)$ and meteorological parameters were compared to the model ones.

4. Discussion of main results

Firstly, we analyse the fields of gradients of atmospheric parameters and their influence on the gradients of the refraction index. This allows to estimate the effects such gradients can have on the retrieval of atmospheric parameters by the RO technique. Then we simulate RO events and determine their errors. Finally, a method for correcting the RO refractivity index profiles (a correction functional) is developed and the functional is derived for the monthly averaged data of February 1997.

4.1. Analysis of atmospheric parameter and refractive index gradients

Using data from the atmospheric model HIRHAM4, we have calculated fields of the spatial gradients of refractivity N, as well as of the atmospheric parameters temperature T, pressure p and humidity w. Fig. 3 provides examples of cross sections and maps of

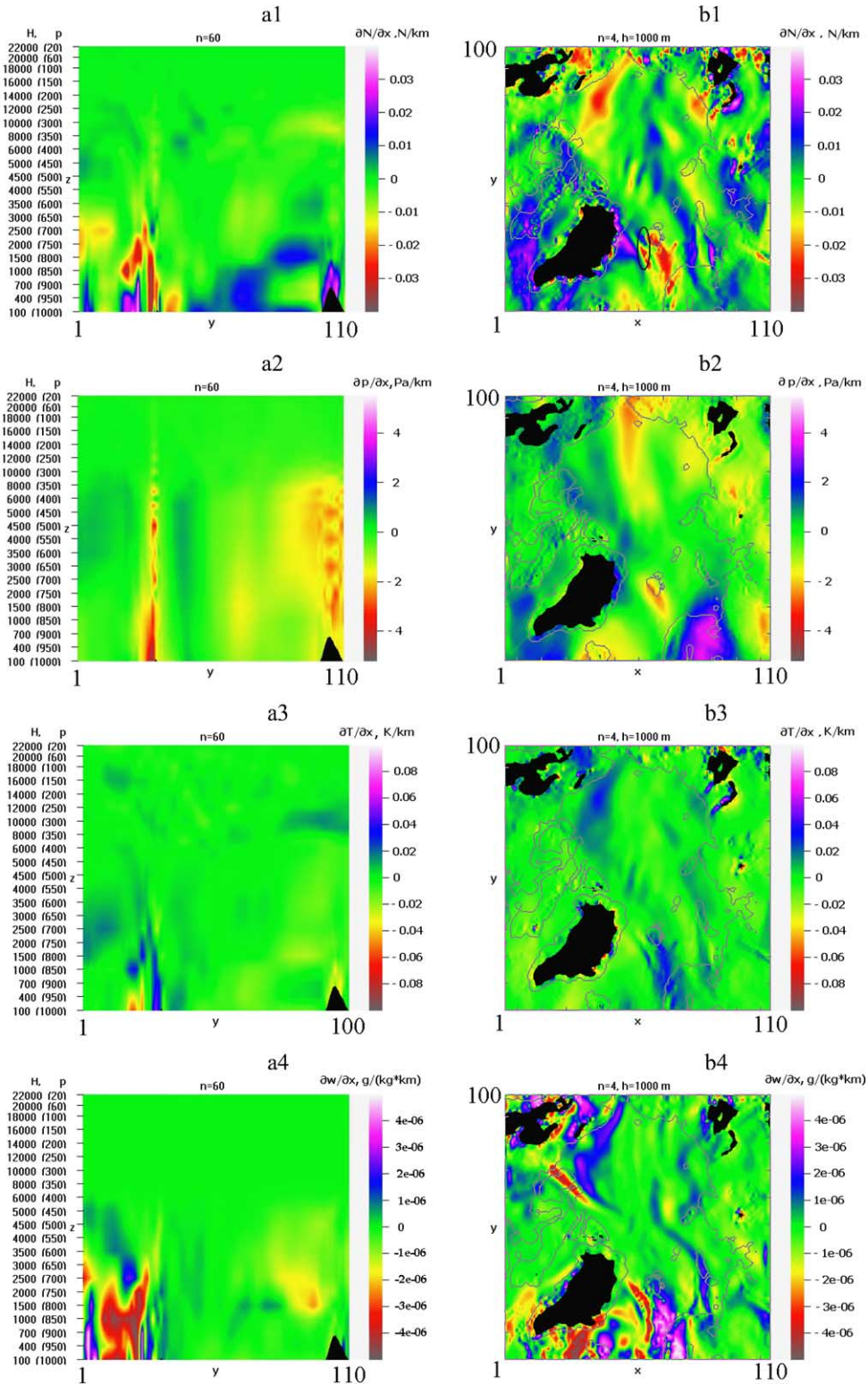

Fig. 3. Cross sections (left row, subplots a1–a4) and horizontal fields at 1000 m altitude (right row, subplots b1–b4) for the gradients of four parameters, namely $\partial N/\partial x$, $\partial T/\partial x$, $\partial p/\partial x$, and $\partial w/\partial x$ as calculated with the HIRHAM4 model for 1 February 1997. The cross sections are along the y-axis at grid points $x = 60$, the altitude scale is indicated in geometric height H [m] and in pressure p [hPa], while the horizontal fields (maps) give the gradients at the model height level 4, which is at 1000 m.

these gradients for the data of 6 UT, 1 February 1997. Figs. 4 and 5 display the errors induced by these gradients on the simulated RO experiments, presented for two height levels in Fig. 4 and for two cross sections in Fig. 5.

We find that the different gradients ∇N, ∇T, ∇p, ∇w have a similar structure. The amplitudes of changes in the refraction index gradient decrease with increasing height. The relief structure (land and ocean areas, coastal lines and mountains) produces traces with specific horizontal and vertical gradients up to the tropopause level at about 10–12 km altitude. The behaviour of the gradients $\partial[n, T, p, w]/\partial y$ is similar to those for $\partial[n, T, p, w]/\partial x$. Monthly averaging distinctly reveals structures stable in time, like the zones associated with the intrusion of warm humid air masses to the Greenland coast and along the Gulf stream. These stable zones can be traced through various height levels and in the maps of simulated errors of the RO experiments, when comparing Figs. 3–5. Table 1 provides numerical values of the gradients with minimum, maximum, and most probable numbers with the occurrence probabilities at altitudes of 1, 3 and 8 km.

The analysis of instantaneous data with the time resolution of 6 h, and for daily, weekly or monthly averaged data shows that the reconstruction errors produced by atmospheric gradient structures can reach 6 K in temperature. The reconstruction errors increase at low altitudes below 4 km, due to the influence of the orography and of the humidity component on the accuracy of reconstruction of other atmospheric parameters. This analysis allows to develop a correction functional for RO data in regions with inhomogeneous structures (see Section 4.3).

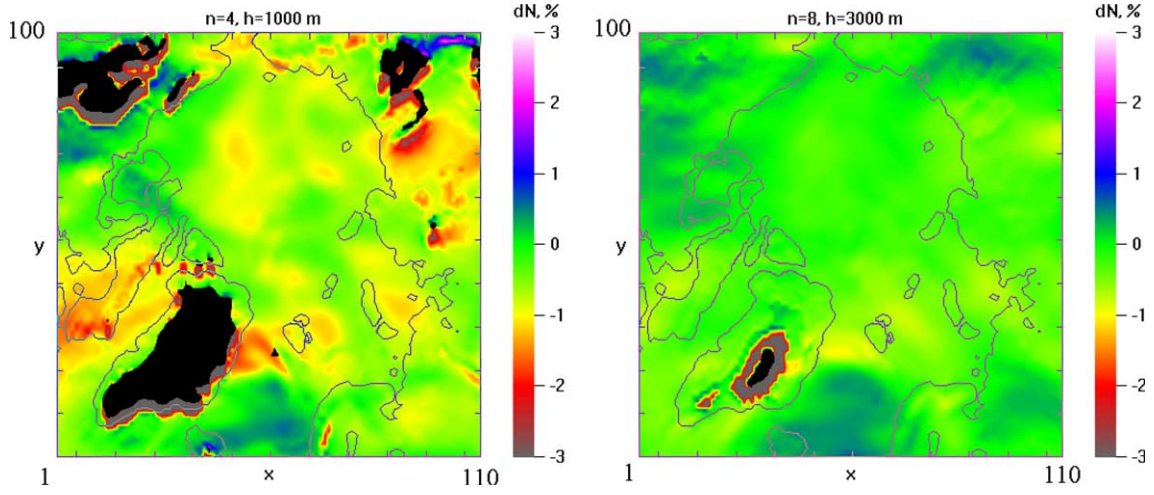

Fig. 4. Horizontal distribution of the relative error of the refraction index at model height levels 4 and 8, corresponding to 1000 m (left plot) and 3000 m (right plot) for the data of 1 February 1997. Black and grey contour lines indicate the Earth's orography.

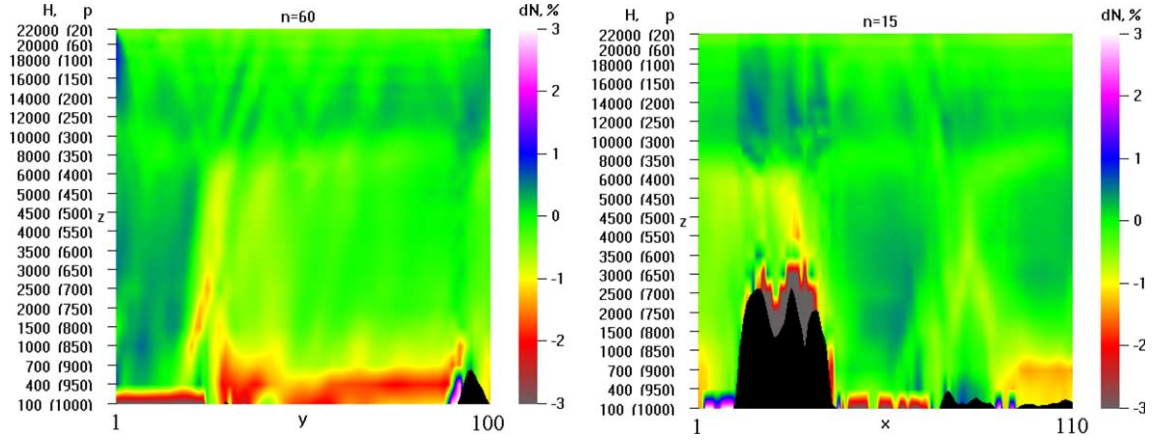

Fig. 5. Altitude distribution of the relative error of the reconstructed refraction index for 1 February 1997 along two cross sections, namely along the y-axis at grid points $x = 60$ (left plot) and along the x-axis at grid points $y = 15$ (right plot). Black shadows sketch the profile of the Earth's surface along the cross sections.

Table 1
Values of studied gradients at altitudes 1, 3, and 8 km (min, max, most probable, rms)

	1 km	3 km	8 km
$\partial N/\partial z$ [N-units/km]			
min/max	−93/3	−29/−19	−21/−13
most probable value	−35	−23.5	−18
rms	9.8	1.8	0.91
$\partial N/\partial x$ [N-units/km]	−0.4/0.5	−0.023/0.037	−0.015/0.017
	−0.0005	−0.0003	−0.001
	0.01	0.005	0.004
$\partial N/\partial y$ [N-units/km]	−0.4/0.6	−0.2/0.3	−0.1/0.047
	−0.0003	−0.0004	−0.001
	0.01	0.006	0.005
$\partial p/\partial z$ [Pa/km]	−120/25	−96/−80	−55/−48
	−11	−89	−52
	32	5	2
$\partial p/\partial x$ [Pa/km]	−11/13	−0.25/0.36	−0.39/0.039
	−0.02	−0.2	−0.03
	0.01	0.01	0.008
$\partial p/\partial y$ [Pa/km]	−12/20	−0.5/0.2	−0.36/0.085
	−0.04	−0.05	−0.05
	0.01	0.012	0.011
$\partial w/\partial z$ [g/kg/km]	−631/39	−0.009/0.063	−4.89E−05/2.46E−06
	−0.2	−0.002	−1E−005
	0.4	0.002	0.005
$\partial w/\partial x$ [g/kg/km]	−6/5	−0.0032/0.0033	−1.44E−04/1.53E−04
	−1E−06	−2E−05	−4E−05
	1.5E−06	8E−04	2E−05
$\partial w/\partial y$ [g/kg/km]	−6/6	−0.022/0.0082	−1.93E−04/2.01E−04
	−2E−06	−2E−05	−2E−05
	1E−03	8E−04	2.7E−05
$\partial T/\partial z$ [K/km]	−9/3	−11/−1	−9/3
	−3	−6	−3
	3.6	1.7	2.3
$\partial T/\partial x$ [K/km]	−0.8/0.5	−0.04/0.03	−0.019/0.02
	−0.0004	0.0004	−0.0001
	0.012	0.008	0.005
$\partial T/\partial y$ [K/km]	−0.4/0.7	−0.03/0.02	−0.07/0.07
	0.0007	−0.0005	−0.0002
	0.013	0.01	0.007

The values of gradients of different atmospheric parameters at the model defined levels are listed in Table 1. From the refractivity index fields n the values of refractivity N has been calculated as $N = (n-1) * 10^6$ (hereby defining the N-unit).

The range of temperature gradients $\partial T/\partial(x,y)$ at 1 km altitude was −0.8 to 0.5 K/km with the most probable value −0.4 and 0.7 K/km respectively for x and y derivatives for the HIRHAM4 data of 1 February 1997. The ranges of pressure gradients $\partial p/\partial(x,y)$ were −11 to 13 Pa/km and −12 to 20 Pa/km, respectively. The variations in the humidity field $\partial w/\partial(x,y)$ range from −6 to 6 g/kg/km. Values for the root mean square (rms) of these values are displayed in Table 1. The spatial localisation of error regions is related to the position of gradient structures, as revealed when comparing Figs. 3–5.

4.2. Modelling of radio occultation events

Errors of the retrieved atmospheric parameters were mapped at the HIRHAM4 model levels in the Arctic region. The analysis makes it possible to propose a physical explanation of the regions where the error exceeds the "background" value. This background error is defined by the error in solving the spherically symmetric problem, which was not higher than 0.2% in these investigations.

The increase in reconstruction errors seems to be caused by two main reasons. First, in a series of cases, the relief shades the atmospheric profiles so that at some altitudes for certain model grid points the reconstruction data are missing. Second, the presence of spherically asymmetric structures due to the influence of moisture and heat inflow into the region causes errors in these regions. In general, the errors in the reconstruction of atmospheric parameters depend on the direction of the sounding.

A wide-scope numerical experiment has been carried out aiming to explore the influence of the factors described. A series of simulations of RO experiments, each consisting of 11,000 single occultation events, were analysed. All possible combinations of GPS satellites and low earth orbital satellites were considered that provide an occultation event corresponding to the model grid points. The ray trajectory direction in the simulation is such that its ground projection coincides with the X- or Y-axis in a curvilinear coordinate frame of the HIRHAM4 model. Each RO experiment contains information about Doppler frequency shift and corresponding refraction angle as a function of the impact parameter over the altitude range 0–80 km with a height increment less than 200 m, which numerically corresponds to the Fresnel radius for the operating frequencies.

Next, the inverse problem, the refraction index profile was reconstructed by means of Abel inversion over a height interval up to 25 km. T, p, and w profiles were non-linearly interpolated to the height levels of the model at the grid points and were compared with the model data at these grid points. The procedures for solving the forward and inverse problems had been applied successively for all sets of the HIRHAM4 model data for February 1997 with 6 h steps in time. Simulations have been carried out for 112 sets of output fields T, p, w of the model. Similar calculations were performed for a series of monthly averaged atmospheric fields.

The structure of the maps shown is similar—both for atmospheric parameter fields and for the reconstruction errors in the described experiment. The map in the horizontal plane (x, y coordinates) represents a two-dimensional cross section at a given height level and contains 11,000 data grid points of the model. Vertical cross sections in z, x and z, y planes are corresponding sections along the remaining coordinate (that is shown as a parameter) and contain 3300 and 3000 data points.

Fig. 4 provides an example of maps of the refractivity error retrieved for two height levels at 1000 and 3000 m, where the sounding path direction is along the y-axis. Fig. 5 shows examples of error maps for two height cross sections in accordance with sounding directions at $x = 60$ (Fig. 5a) and $y = 15$ (Fig. 5b). The increasing errors in some regions are in accordance with the existing gradient structures in the atmospheric data.

The analysis of the HIRHAM4 model data shows, that fluctuations in the refraction index above 3 km are caused mainly by variations in the temperature field. Due to the low Arctic humidity content it follows from formula (4) that at height levels above 3 km for relative errors the relationship $|\delta N_{\text{error}}|/N \approx |\delta T_{\text{error}}|/T$ is valid.

Figs. 4 and 5 portray typical spatial distributions of errors at several height levels. It can be seen that errors decrease with increasing height. Note that the errors reach 1% within areas containing orographic perturbations and, as a result, disturbances in atmospheric fields.

4.3. Construction of the correction functional

The need to improve the occultation retrieval can be reduced to the problem of finding the correcting functional. If $\mathbf{T}$ represents the ray tracing operation to obtain a vertical profile of the refraction angle $\alpha(h)$ from a given refraction index field $N(\vec{r})$ and $\mathbf{A}$ denotes the inverse operation (6) to obtain a retrieved vertical profile of refraction index N^{ret} from a given refraction angle $\alpha(h)$, we can write

$$N^{\text{ret}} = \mathbf{A}\alpha(h) = \mathbf{AT}N(\vec{r}).$$

Local errors of reconstruction $\delta N = N - N^{\text{ret}}$ for the given profile $r = \{x_i, y_j, h\}$ are defined as $\delta N = N - N^{\text{ret}} = (\mathbf{I} - \mathbf{AT})N$ where $\mathbf{I}$ is unity operator. However, we cannot determine δN because the field N is unknown. Therefore one should state a problem of finding an approximation $\delta N^{\text{corr}} \cong \delta N$. It should be mentioned that δN is defined only by transverse gradients of the refraction field. Indeed, when N is divided into a spherically symmetric part N_0 and an addition ΔN associated with transverse gradients, the equality $\delta N = (\mathbf{I} - \mathbf{AT})N = (\mathbf{I} - \mathbf{AT})\Delta N$ is valid since $(\mathbf{I} - \mathbf{AT})N_0 = 0$. If the function $\Delta N = N - N_0$ is close to $\Delta N^{\text{mod}} = N^{\text{mod}} - N_0^{\text{mod}}$, that is, the structure of model gradients N^{mod} follows the major features of real field gradients, one can use $\delta N^{\text{corr}} = N^{\text{mod}} - \mathbf{AT}N^{\text{mod}}$ as an approximation of δN. Let us name this approximation $\delta N^{\text{corr}} = N^{\text{mod}} - \mathbf{AT}N^{\text{mod}}$ a correction functional. The term "functional" is used here because δN^{corr} depends on both the refraction field and on the direction of sounding. The correction functional makes it possible to perform a correction of the retrieved vertical profiles using the model data and ray tracing data.

$$\begin{aligned} N &= N^{\text{ret}} + \delta N \cong N^{\text{ret}} + \delta N^{\text{corr}} \\ &= N^{\text{ret}} + N^{\text{mod}} - \mathbf{AT}N^{\text{mod}}. \end{aligned} \tag{7}$$

The quality of correction will depend on how adequate the model is and how close the structure of model gradients is to that of real field gradients.

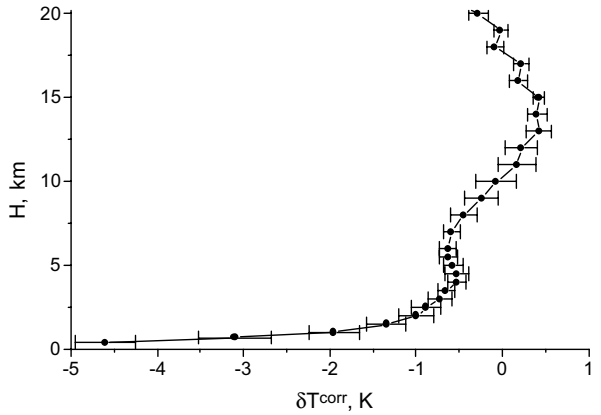

Fig. 6. Profile of the monthly averaged correction of the retrieved temperature for February 1997 at a point close to the centre of the Arctic ($x = 45$, $y = 70$). Thin horizontal lines give the rms values.

The HIRHAM model is quite able to describe the monthly averaged distributions of atmospheric parameter fields and the refraction index field. The error in temperature, for example, is generally less than 1 degree (Rinke et al., 1999). We apply the data from this model to calculate time averaged corrections using relation (7) in a temporally averaged form. If the correction values considerably exceed the rms of the time averaged profiles, then the correction will not be efficient. In Fig. 6 an example is shown of monthly averaged correction for February 1997 of the retrieval temperature for a point close to the centre of the Arctic ($x = 45$, $y = 70$). Here the rms is not higher than 0.2 K although errors at lower levels reach several degrees. In most cases (about 70%) of such time averaging the rms did not exceed 0.5,...,1 K with correction values of up to 6 K.

For instantaneous values of atmospheric fields the correction is not always efficient since the simulation of instantaneous atmospheric fields by the HIRHAM4 model is contaminated by different strong biases in different parts of the model area. However, here one can apply the averaging (7) in the space domain. As is well known, the refraction field N is reconstructed as "averaged" along the ray of about 600 km around the ray perigee point. Fig. 7 shows an example of the correction of the vertical temperature profile after spatial averaging within a strip ($x = 65$–66, $y = 20$–32). Here the correction works efficient at lower levels. Such correction of instantaneous values of atmospheric parameters are useful only in rather extended regions (larger than 500 km), such as the centre of the Arctic or along the Gulf stream.

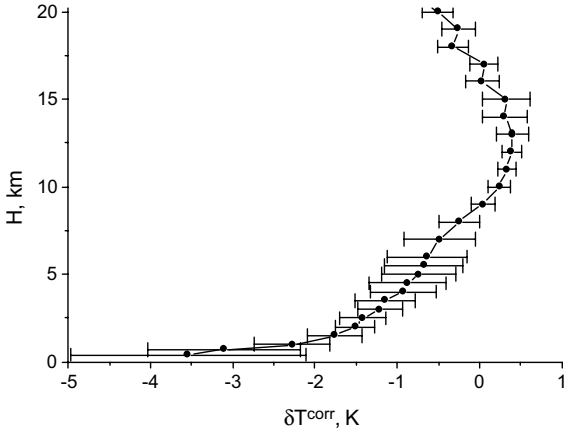

Fig. 7. Profile of the temperature correction after a spatial averaging along a cross section (x: 65–66, y: 20–32), thin horizontal lines give the rms values.

5. Summary

An interpretation of RO data combined with a regional atmospheric model which successfully simulates atmospheric large and mesoscale structures has been proposed and tested. The irregular non-spherical structure of the atmosphere as the medium of radio signal propagation has a key effect on the reconstruction accuracy of vertical profiles of atmospheric parameters studied in experiments with GPS systems. This cumbers the interpretation, how mesoscale variations influence the profiles of atmospheric parameters.

The data obtained in RO experiments contain errors that are spatially localised and associated with gradients in atmospheric data. The local errors in profiles of temperature, pressure, and refractivity obtained by this RO method can reach 2%. This corresponds for example to an error of 6 K in temperature.

If the spatial size and amplitude of the mesoscale atmospheric structures are known, one can construct a non-linear functional dependency of the error of the retrieved refractivity using the spatial and amplitude parameters of the irregularity and its gradients. This functional can be constructed from instantaneous model outputs, as well as from temporally averaged fields of refractivity. Such an averaged correction functional can be constructed from data averaged over time intervals ranging from days to months within a special region. Here such a functional has been constructed from the data of the HIRHAM4 model for the Arctic region for the time averaged fields of February 1997. The correction functional derived from monthly averaged data reduced the retrieval errors of refractivity, temperature, and pressure in the troposphere. The retrieval errors of temperature are reduced to less than 1 K. The application of such a functional to experimental data depends on the reliability of the model with respect to the real atmospheric mesoscale structures. Such an approach is justified in regions like the Arctic where the regional atmospheric model has been successfully validated and other data are sparse.

Acknowledgements

Financial support for this study was provided by the strategy fund project "GPS Atmosphere Sounding" of the Helmholtz Association of German Research Centers. The HIRLAM system was developed by the HIRLAM project group, a cooperative project of the national weather services in Denmark, Finland, Iceland, Ireland, Netherlands, Norway, Spain, and Sweden. We would like to particularly thank two anonymous reviewers for very helpful suggestions and comments.

References

Ahlberg, J., Nilson, E., Walsh, J., 1967. The Theory of Splines and Their Applications. Academic Press.

Bean, B.R., Dutton, E.J., 1968. Radio Meteorology. New York.

Bengtsson, L., Gorbunov, M.E., Sokolovsky, S.V., 1996. Space refractive tomography of the atmosphere. Modeling of direct and inverse problems. Report No. 210, Max-Planck Institute for Meteorology, Hamburg.

Bilitza, D. (Ed.), 1990. International Reference Ionosphere 1990, NSSDC 90-22, Greenbelt, MD.

Dethloff, K., Rinke, A., Lehmann, R., Christensen, J.H., Botzet, M., Machenhauer, B., 1996. Regional climate model of the Arctic atmosphere. J. Geophys. Res. 101, 23401–23422.

Dethloff, K., Schwager, M., Christensen, J.H., Kiilsholm, S., Rinke, A., Dorn, W., Jung-Rothenhäusler, F., Fischer, H., Kipfstuhl, S., Miller, H., 2002. Recent Greenland accumulation estimated from regional climate model simulations and ice core analysis. J. Climate 15, 2821–2832.

Fjeldbo, G., Eshleman, V.R., 1965. The bistatic radar-occultation method for the study of planetary atmospheres. J. Geophys. Res. 70, 3217–3226.

Forsythe, G.E., Moler, C.B., Malcolm, M.A., 1977. Computer Methods for Calculations. Prentice-Hall, Inc.

Gibson, J.K., Kalberg, P., Uppala, S., Hernandez, A., Nomura, A., Serrano, E., 1997. ERA description. ECMWF Re-Analysis Project Report, Series 1, 72 pp.

Gorbunov, M.E., 1994. The optimal accuracy for radio occultation technique in atmosphere sounding. Izv. RAN, FAO 30 (6), 776–778 (in Russian).

Gorbunov, M.E., 2001. Radio holographic methods for processing radio occultation data in multipath regions. Report N 01-02, Danish Meteorological Institute.

Gorbunov, M.E., Gurvich, A.S., 1998. Microlab-1 experiment: multipath effects in the lower troposphere. J. Geophys. Res. 103, 13819–13826.

Gorbunov, M.E., Kornblueh, L., 2001. Analysis and validation of GPS/MET radio occultation data. J. Geophys. Res. 106, 17161–17170.

Gorbunov, M.E., Sokolovskiy, S.V., 1993. Remote sensing of refractivity from space for global observations of atmospheric parameters. Report No. 119, Max-Planck Institute for Meteorology, Hamburg.

Hajj, G.A., Romans, L.J., 1998. Ionospheric electron density profiles obtained with the Global Positioning System: results from GPS/MET experiment. Radio Sci. 33, 175–190.

Healy, S.B., 2001. Radio occultation bending angle and impact parameter errors caused by horizontal refractive index gradients in the troposphere: a simulation study. J. Geophys. Res. 106, 11875–11890.

Healy, S.B., Eyre, J.R., 2000. Retrieving temperature, water vapour and surface pressure information from refractive-index profiles derived by radio occultation: a simulation study. Q. J. R. Meteorol. Soc., 1661–1683.

Kattsov, V.M., Walsh, J.E., Rinke, A., Dethloff, K., 2000. Atmospheric climate models: simulations of the Arctic Ocean fresh water budget components. In: Lewis, E.L. (Ed.), The Freshwater Budget of the Arctic Ocean. Kluwer Academic, pp. 209–247.

Kursinski, E.R., Hajj, G.A., Hardy, K.P., Romans, L.J., Schofield, J.T., 1995. Observing tropospheric water vapor by radio occultation using the global positioning system. Geophys. Res. Lett. 22, 2365.

Kursinski, E.R., Hajj, G.A., Schofield, J.T., Linfield, R.P., Hardy, K.R., 1997. Observing Earth's atmosphere with radio occultation measurements using the global positioning system. J. Geophys. Res. 102, 23429–23465.

Leitinger, R., Ladreiter, H.-P., Kirchengast, G., 1997. Ionosphere tomography with data from satellite reception of Global Navigation Satellite System signals and ground reception of Navy Navigation Satellite System signals. Radio Sci. 32, 1657–1669.

Palmer, P.I., Barnett, J.J., Eyre, J.R., Healy, S.B., 2000. A nonlinear optimal estimation inverse method for radio occultation measurements of temperature, humidity, and surface pressure. J. Geophys. Res. 105, 17513–17526.

Phinney, R.A., Anderson, D.L., 1968. The radio occultation method for studying planetary atmospheres. J. Geophys. Res. 73, 1819–1827.

Rees, D. (Ed.), 1988. CIRA 86 Adv. Space Res. 8 (5–6).

Rinke, A., Dethloff, K., 2000. On the sensitivity of a regional Arctic climate model to initial and boundary conditions. Climate Res. 14, 101–113.

Rinke, A., Dethloff, K., Christensen, J.H., Botzet, M., Machenhauer, B., 1997. Simulation and validation of Arctic radiation and clouds in a regional climate model. J. Geophys. Res. 102, 29833–29847.

Rinke, A., Dethloff, K., Spekat, A., Enke, W., Christensen, J.H., 1999. High resolution climate simulations over the Arctic. Polar Res. 18, 143–150.

Rinke, A., Lynch, A.H., Dethloff, K., 2000. Intercomparison of Arctic regional climate simulations: case studies of January and June 1990. J. Geophys. Res. 105, 29669–29683.

Rocken, C., Anthes, R., Exner, M., Hunt, D., Sokolovsky, S., Ware, R., Gorbunov, M.S., et al., 1997. Analysis and validation of GPS/MET data in neutral atmosphere. J. Geophys. Res. 102, 29849–29866.

Schreiner, W.S., Sokolovsky, S., Rocken, C., Hunt, D.C., 1999. Analysis and validation of GPS/MET radio occultation data in the ionosphere. Radio Sci. 34, 949–966.

Syndergaard, S., 2000. On the ionosphere calibration in GPS radio occultation measurements. Radio Sci. 35, 865–883.

Vorob'ev, V.V., Krasilnikova, T.G., 1993. The estimation of reconstruction accuracy atmospheric refractivity index by Doppler shift on frequencies used by the NAVSTAR system. Rep. Acad. Sci. USSR, Phys. 29, 626–633 (in Russian).

Wallace, J.M., Hobbs, P.V., 1977. Atmospheric Science. An Introductory Survey. Academic Press.

Zakharov, V.I., Kunitsyn, V.E., 1998. Modeling of ionosphere's and protonosphere's influence on the accuracy of atmospheric parameters reconstructions by radio occultation technique. Moscow Univ. Phys. Bull. 53, 53–59.

Zakharov, V.I., Kunitsyn, V.E., 1999. Multipath influence on the profiling accuracy in radio occultation experiments. Moscow Univ. Phys. Bull. 54, 46–52.

Zou, X., Vandenberghe, F., Wang, B., Gorbunov, M.E., Yu, M., Kuo, Y.-H., Sokolovsky, S., Chang, J.C., Sela, J.G., Anthes, R.A., 1999. A ray-tracing operator and its adjoint for the use of GPS/MET refraction angle measurements. J. Geophys. Res. 104, 22301–22318.